JOURNAL OF AGRICULTURAL AND FOOD CHEMISTRY

pubs.acs.org/JAFC Article

Nobiletin Attenuates DSS-Induced Intestinal Barrier Damage through the HNF4α-Claudin-7 Signaling Pathway

Xiang Wen, Hui Zhao,* Liwen Wang, Liang Wang, Gang Du, Wenqiang Guan, Jianfu Liu, Xiaocang Cao, Xiaohua Jiang, Jingrui Tian, Meiyan Wang,* Chi-Tang Ho, and Shiming Li*

Cite This: J. Agric. Food Chem. 2020, 68, 4641−4649 Read Online

ACCESS | Metrics & More | Article Recommendations | Supporting Information

ABSTRACT: The intestinal epithelium barrier functions to protect human bodies from damages such as harmful microorganisms, antigens, and toxins. In this study, we evaluated the protective effect and molecular mechanism of a dominant polymethoxyflavone nobiletin (NOB) from tangerine peels on intestinal epithelial integrity. The results from transepithelial electrical resistance (TEER) suggested that NOB pretreatment counteracts epithelial injury induced by inflammatory cytokines (TEER value in 48 h: vehicle, 135.6 ± 3.9 Ω/cm^2; TNF-α + IL-1β, 90.7 ± 0.5 Ω/cm^2; 10 μM NOB + TNF-α + IL-1β, 126.1 ± 0.8 Ω/cm^2; 100 μM NOB + TNF-α + IL-1β, 125.3 ± 0.5 Ω/cm^2. $P < 0.001$). Clinical and pathological test results suggested that administration of NOB effectively alleviates intestinal barrier injury induced by dextran sulfate sodium (DSS) as evidenced by the length of colon villi on day 7 (control, 253.7 ± 4.8 μm, DSS 131.6 ± 4.6 μm, NOB + DSS, 234.5 ± 5.1 μm. $P < 0.001$). Interestingly, when screening tight junction molecules for intestinal barrier integrity, we observed that independent treatment with NOB sharply increased claudin-7 levels (ratio of claudin-7 over GAPDH: control, 1.0 ± 0.06; DSS, 0.02 ± 0.001; NOB + DSS, 0.3 ± 0.07. $P < 0.001$), which was previously suppressed upon DSS stimulation. Furthermore, hepatocyte nuclear factor 4α (HNF-4α) transcriptional regulation of claudin-7 contributed to intestinal barrier homeostasis. Therefore, our study suggests potential intestinal protective strategies based on polymethoxyflavones of aged tangerine peels.

KEYWORDS: *claudin-7, HNF-4α, intestinal epithelial barrier, nobiletin, tangerine peels*

INTRODUCTION

The intestinal epithelium barrier regulates the passage of substances including water, ions, macromolecules, and even organisms between the intestinal lumen and underlying tissue compartments.[1] Intestinal integrity is crucial to maintain homeostasis, and the leaky barrier promotes intestinal dysfunction and pathogenesis. In epithelial tissues, the tight junctions (TJs) are clearly critical for the formation of intestinal barriers by inducing epithelial morphogenesis and regulating permeability.[2] TJs are multiprotein complexes mainly composed of claudins, occludin, and zonula occludens, which are distributed near the intercellular spaces between adjacent epithelial cells.[3] Specifically, TJ proteins in the gut lumen are responsible for modulating the paracellular permeability and transportation of solutes and ions. The malfunction of TJs is closely associated with infection, inflammation, obesity, and even autoimmune diseases.[4] Claudin-7, a major TJ component in epithelial cells, is indispensable in controlling Wnt/β-catenin signaling-dependent intestinal epithelial stem cell survival, self-renewal, and cell differentiation.[5]

Aged peels of tangerine (*Citrus reticulata* Blanco) have been used as food and herbal ingredients for several centuries in Southeast Asia. Tangerine peels are a rich source of polymethoxyflavones (PMFs) such as nobiletin (5,6,7,8,3′,4′-hexamethoxyflavone, NOB), which is exclusively identified in citrus genus.[6,7] PMFs have been reported to be involved in anti-inflammation, anticancer, antioxidant, and antiallergy properties.[8−11] Notably, an increasing number of studies has focused on the protective function of NOB on the intestinal epithelium.[12] For example, NOB was proved to alleviate symptoms and inflammatory markers in chronic murine colitis.[13] Wu et al. demonstrated that NOB and its metabolites suppressed colitis-associated colon carcinogenesis by down-regulating iNOS, inducing antioxidative enzymes and arresting cell cycle progression.[14] The established intestinal protective mechanisms of NOB and its colonic metabolites are involved in classic signaling pathways, including that of nuclear factor erythroid 2-related factor (Nrf2),[14] Akt, and nuclear factor-kappa B (NF-κB).[15] In addition, other studies also proved that NOB can regulate several types of TJ proteins such as claudin-2, occludin, ZO-1,[12] and claudin-5.[16] However, whether and how NOB participates in intestinal barrier integrity by modulating TJ molecules remained to be explored further.

Herein, we report that NOB can effectively alleviate dextran sulfate sodium (DSS)-induced intestinal epithelial injury; the TJ molecule claudin-7 in intestinal epithelial tissue plays a vital role in intestinal barrier protection; and the mechanism that claudin-7 expression is driven by nuclear transcription factor

Received: February 21, 2020
Revised: March 28, 2020
Accepted: April 5, 2020
Published: April 5, 2020

https://dx.doi.org/10.1021/acs.jafc.0c01217
J. Agric. Food Chem. 2020, 68, 4641−4649

hepatocyte nuclear factor 4α (HNF-4α) in intestinal epithelial cells has been confirmed.

MATERIALS AND METHODS

Chemicals. Nobiletin with a purity of 98.5% characterized by high-performance liquid chromatography and proton nuclear magnetic resonance was isolated in house from aged tangerine peels according to previously described method.[17] The toxic effects of NOB have been assessed by MTT assay and liver enzyme measurement. The results were illustrated in Figures S1 and S2.

Regents, Cell Culture, and Differentiation. Details on the regents, antibodies, cytokines, kits, and recombinant DNA plasmids are provided in Table S1 unless otherwise indicated. The cells used in the experiments, including 293T cells, human HT-29 colorectal cancer cells, Caco-2 cells, and IEC-6 rat intestinal epithelial cells, were obtained from the American Type Culture Collection and cultured in DMEM containing 10% foetal bovine serum, 2 mg/L insulin (for IEC-6 cells only), and 1% penicillin at 37 °C with a humidified 5% CO_2 atmosphere. IEC-6 or Caco-2 cells (1×10^5 cells/well) were seeded on a sterile 24-well culture plate and cultured while the medium was changed daily. The transepithelial electrical resistance (TEER) value of IEC-6 model was measured at day 8 and that of Caco-2 model was measured at day 22. HT-29 cells were seeded at a density of 5×10^5 cells/well in a 6-well plate and harvested for cell transfection assay 24−48 h later. For the ChIP assay, HT-29 cells were seeded at high density (2×10^6 to 4×10^6) in 10 cm culture dishes and harvested after 24 h. For the luciferase assay, HEK 293T cells (10^4 cells/well) were seeded on 96-well plates, transfected the 12 h later by luciferase reporter constructs, and harvested after 48 h.

Animals. Male C57BL/6J mice, 8−10 weeks old, weighing 21−23 g, were purchased from Vital River Laboratory Animal Technology Co., Ltd. (China) and allowed to acclimate for 1 week before the start of the experiment. All of the mice were housed under controlled humidity (65−70%), light (12 h light/dark cycle), and temperature (23 °C). All animal experiments were approved by the ethics committee of Tianjin University of Commerce, and Certification Materials will be provided upon request.

The mice were randomly separated into three groups (12 mice in each group): control mice, mice administered with DSS only, and mice receiving diets containing NOB (0.01% or 0.25 mmol NOB in one kg of diet wt/wt). The control group drank water without DSS, but the other groups had ad libitum access to deionized water containing 3% (0.6−0.8 mM, w/v) DSS. Body weight, food intake, and disease activity index (DAI) scoring were recorded daily.[18,19] Mice were sacrificed, and intestinal tissue samples were collected on day 7.

Transepithelial Electrical Resistance. TEER values (Ω/cm^2) were monitored with an EVOM II epithelial voltohmmeter (World Precision Instruments, Sarasota, FL, USA) according to a method we previously used.[20] IEC-6 or Caco-2 cells were planted into the upper Transwell 0.33 cm^2 chamber (Corning Costar, NY, USA) at a density of 1×10^5 cells/mL, and 1 mL of medium was added to the lower chamber. When the cells reached 90% confluence on the plate, NOB was added for a 6 h treatment, following a treatment with 100 ng/mL of TNF-α and 50 ng/mL of IL-1β for additional 48 h prior to TEER measurement.

Fluorescein Isothiocyanate-Dextran Permeability Experiments. Seven days after the DSS treatment, the mice were orally administered 0.6 mg/g fluorescein isothiocyanate (FITC)-dextran 4 h prior to sacrifice. Serum samples were obtained by centrifuging the blood samples at 1000 g/min and 4 °C for 10 min. A standard curve was generated using mouse serum from age-matched C57BL/6 male mice that was spiked with increasing amounts of FITC dextran. Samples were added to totally black 96-well plates to detect 528 nm emission at 485 nm excitation.

Cell Transfection. HNF-4α targeting siRNA (HNF-4α target sequences: GGCTCAAGCAGGAAATCGA) and a negative control siRNA were synthesized by GenePharma (Shanghai, China) and transfected with Lipofectamine 2000 reagent according to the kit protocol. After 48 h of transfection, the cells were exposed to the indicated concentration of NOB for 24 h and harvested for RNA extraction and qPCR analysis.

Quantitative Reverse Transcription qPCR Analysis. RNA extraction, 1st strand cDNA synthesis, and reverse transcription polymerase chain reaction were performed as described previously.[20] qPCR was carried out using a LightCycler 96 (Roche, USA) and reagent mixture. The primers used are listed in Table S2.

H&E-Stained Sections and Immunohistochemistry. Tissue fixed in 4% (w/v) paraformaldehyde in phosphate-buffered saline (PBS) was prepared for light microscopy, and 5 μm-thick sections were stained with H&E to study histologic changes. The H&E-stained sections were analyzed blindly by a veterinary pathologist. The length of the villi is the distance from the crypt mouth to the tip of the villi. Four different fields were selected in each tissue section, and the average value was taken to reduce the potential impact of patchy necrosis.

Immunohistochemistry staining was carried out according to the kit instructions. Five-micron-thick tissue sections were stained with antibodies against claudin-7, HNF-4α and iNOS (Figure S3).

Western Blotting. Whole colon tissue (50 mg) was homogenized in 1 mL of ice-cold RIPA buffer containing 0.1% phenylmethylsulfonyl fluoride. Immunoblotting for claudin-7 and HNF-4α was performed as previously described.[21,22]

Chromatin Immunoprecipitation Assays. Chromatin immunoprecipitation (ChIP) assays were performed using a sonication ChIP kit with minor modifications. HT-29 cells were cross-linked with 1% formaldehyde and quenched with glycine. The cells were then collected and placed in ice-cold, phosphate-buffered saline containing protease inhibitors. Chromatin was isolated by adding cell lysis buffer, and DNA was sheared into fragments of 200−500 bp by sonication with a 1/8 in. Micro tip during a 30 min of 15 s on/15 s off 30% sonication cycle. Next, the DNA samples were precipitated with anti-HNF-4α or human IgG used as a control. The primers for ChIP are listed in Table S2.

Luciferase Assays. Luciferase reporter constructs (Table S3), including mutated constructs and wild-type constructs, were established according to a previous report.[4] HEK 293T cells were transfected with 200 ng of claudin-7—pGL4.10 vector per well [or equimolar amounts of mut1-pGL4, mut2-pGL4, mut1 + 2- pGL4, pGL4.10 (empty vector)] and 0.04 mg of pRL-TK per well, which was used as a control to determine transfection efficiency. Twelve hours after the transient transfection, the cells were incubated with or without nobiletin (100 μmol/L) for 6 h and then treated with 100 ng/mL TNF-α and 0.5 ng/mL LPS for 48 h. Samples were generated in triplicate in 96-well tissue culture plates, and each well was transfected at the same time because older cultures are resistant to transfection. Luciferase activity was measured, and reporter activity was determined using a dual-luciferase reporter assay system according to the manufacturer's protocol.

Immunofluorescence Staining and Confocal Microscopy. The mouse colon-tissue sections were fixed with 4% (w/v) paraformaldehyde and embedded in paraffin. The tissues were sectioned (5 mm-thick), deparaffinized, and blocked with 3% bovine serum albumin in PBS, followed by incubation with anti-claudin-7 antibody and anti-HNF-4α for 12 h at 4 °C. Alexa Fluor 488 and Alexa Fluor 546 were used as secondary Abs (1:50 dilution) for 1 h at room temperature. The nuclei were stained with DAPI (10 μg/mL). Images of immunofluorescent sections were captured using a Nikon A1R confocal microscope (100× oil immersion objective).

Statistical Analysis. All data were obtained from at least three independent experiments and expressed as the mean ± SEM unless otherwise indicated. The experimental data were analyzed using GraphPad Prism software (San Diego, CA, USA). One-way ANOVA testing was used to assess differences between groups, followed by Dunnett's test. $P < 0.05$ was considered statistically significant.

RESULTS

NOB Maintained Intestinal Epithelial Function. To check the potential protection of NOB on intestinal barrier

https://dx.doi.org/10.1021/acs.jafc.0c01217
J. Agric. Food Chem. 2020, 68, 4641−4649

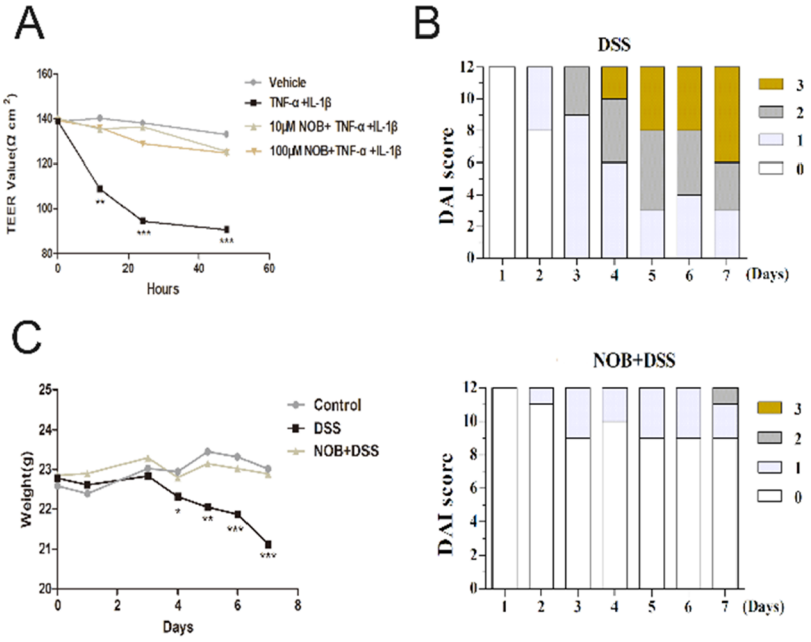

Figure 1. NOB maintained intestinal epithelial function. (A) Changes in the TEER value across IEC-6 monolayers over time. Cells were treated with NOB/vehicle prior to TNF-α and IL-1β. Transepithelial resistance readings at 12, 24, and 48 h after treatment. (B) DAI scores of mice during 7 days of DSS-induced colitis experiments: 0, body weight loss <2%, normal faeces and no rectal bleeding; 1, body weight loss 2−5%, softer stool and weak hemoccult; 2, body weight loss 5−10%, moderate diarrhea and visual blood in stool; 3, body weight loss 10−15%, diarrhea and fresh rectal bleeding. (C) Changes in body weight of mice in different treatment groups within 7 days. DSS concentration is 3% (0.6−0.8 mM), NOB concentration is 0.25 mmol NOB in 1 kg of diet or 0.01% (wt/wt). All error bars represent SEM (*P < 0.05; **P < 0.01; ***P < 0.001).

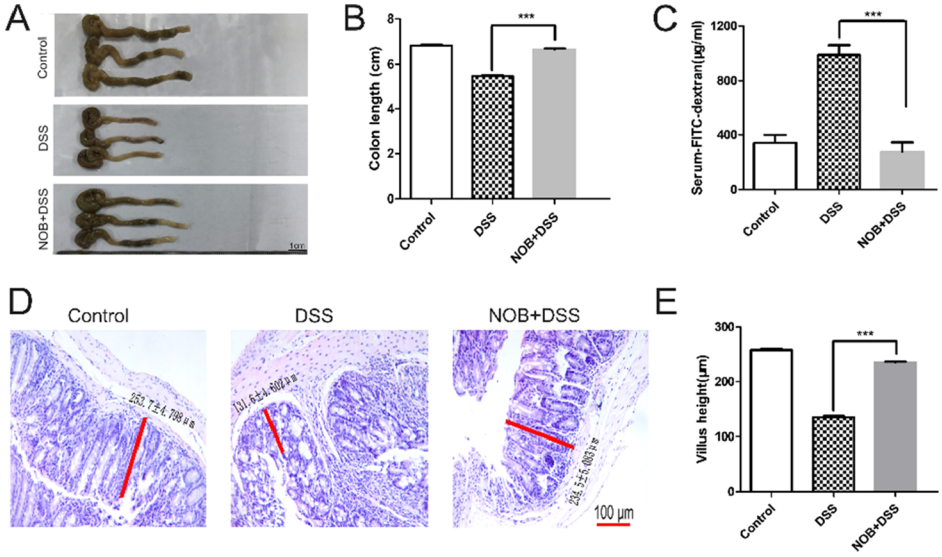

Figure 2. NOB protected colon integrity. (A) After mice were sacrificed on day 7, colon tissue samples were dissected and assessed; (B) measured the length of three colons in each group; (C) epithelial integrity was assessed by serum FITC-dextran on day 7; (D) cross-sections of the mouse colon were taken 7 days after DSS treatment. In NOB-treated and nontreated mice, colonic responses to DSS were measured (H&E stained cross sections; ×20 objective). Scale bars, 100 μm; (E) comparison of villi lengths of each group by using Leica LAS EZ software. DSS concentration is 3% (0.6−0.8 mM), NOB concentration is 0.25 mmol NOB in one kg of diet or 0.01% (wt/wt). All error bars represent SEM (***P < 0.001).

function, we first determined the TEER in IEC-6 rat colon cells and Caco-2 cells (Figure S4). As shown in Figure 1A, NOB reversed the epithelial injury induced by TNF-α and IL-1β stimulation. To strengthen the confirmation, we then explored the treatment potential NOB in a DSS-induced intestinal epithelial damage model. As expected, the DAI scores showed that mice with the administration of NOB exhibited the improved health status than mice treated with only DSS (Figure 1B). Likewise, the body weight recovery of the mice in the DSS group was dramatically lower than that of the NOB group on day 7 (Figure 1C). These results indicated that NOB can effectively maintain the function of the intestinal mucosa.

NOB Protected Colon Integrity. To investigate the protection of intestinal epithelial integrity by NOB, we observed that the colon was shortened to a markedly lower extent in both the NOB group compared to the colon shortening observed in the DSS group mice (Figure 2A,B). Furthermore, lower levels of serum FITC-dextran were leaked

https://dx.doi.org/10.1021/acs.jafc.0c01217
J. Agric. Food Chem. 2020, 68, 4641−4649

from the intestinal barrier of mice that had received the NOB or treatment compared to the level leaked in the mice treated only with DSS (Figure 2C). Consistent with these observations, pathological colon slides indicated that NOB treatment counteracted DSS-induced integrity destruction, as indicated in the intestinal mucosal architecture (Figure 2D), (near) normal length of the villi (Figure 2E), and reduced level of the inflammatory marker iNOS (Figure S1). Taken together, these results suggested that NOB effectively improved DSS-induced intestinal barrier dysfunction.

NOB Increased the Expression of Claudin-7 in Mouse Colon. Having confirmed the maintenance of intestinal integrity, we then investigated the potential mechanisms regarding NOB protection. Because of the key role of TJ proteins in intestinal stability,[23] claudins, particularly claudin-1, -2, -3, -7, and -10, attracted our attention because of their close association with crypt-villus barrier architecture and intestinal epithelial differentiation.[24] To our excitement, of the TJs we checked, claudin-7 was the most sensitive molecule to respond to stimuli in the intestines of both NOB- treated mice (Figure S5). This observation was further supported by the evidence from the RT-PCR and the immunohistochemistry tissue samples (Figure 3A–C) and was consistent with a previous report that mice lacking claudin-7 present with destroyed mucosal barriers with ulceration.[25] Thus, our data suggested that the increased claudin-7 content may have been involved in the intestinal integrity modulation by NOB.

Modulation of Claudin-7 by HNF-4α Was Involved the Intestinal Protection Conferred by NOB. Having determined that claudin-7 transcription was stimulated by NOB in mice, we then attempted to determine the potential for modulated claudin-7 expression in intestinal epithelium. In theory, epithelial integrity depends on transcriptional mechanisms to properly establish the epithelial barrier through TJ components, which are mainly controlled by nuclear receptors.[26] Claudin-7 is usually regulated by the nuclear receptor HNF-4α occupying its promoter, and HNF-4α has an almost identical distribution in gut epithelial as claudin-7 can regulate cell junctions, metabolism, and proliferation.[4,26,27]

To confirm the regulation of HNF-4α on claudin-7 during NOB treatment, we first examined whether the expression levels of HNF-4α and claudin-7 were consistent in mouse colon. As expected, our results indicated that HNF-4α was positively correlated with claudin-7 in terms of pathological severity. For example, colon biopsy samples showed that the addition of NOB to mice sharply reversed the downregulation of both HNF-4α (Figure 4A,B) and claudin-7 (Figure 3A,B) in mice that received DSS treatment.

In addition, the results of western blotting (Figure 5A,B) are consistent with that of immunohistochemistry. Compared with the DSS group, NOB can significantly ($P < 0.001$) increase the expression of claudin-7 and HNF-4α in mouse colon. Therefore, the expression of claudin-7 and HNF-4α in mouse colon is consistent and the regulation of claudin-7 by HNF-4α is related to the intestinal protection of NOB.

Increased Claudin-7 Promoter Activity upon NOB Stimulation Was Mediated by Nuclear Receptor HNF-4α. As our in vivo data indicated a clear correlation between HNF-4α and claudin-7 upon stimulation with NOB, we then investigated whether the modulation of claudin-7 by NOB, a representative bioactive agent from aged tangerine peels, in colon cells was related to HNF-4α expression. In line with our in vivo observation, the level of claudin-7 mRNA was increased

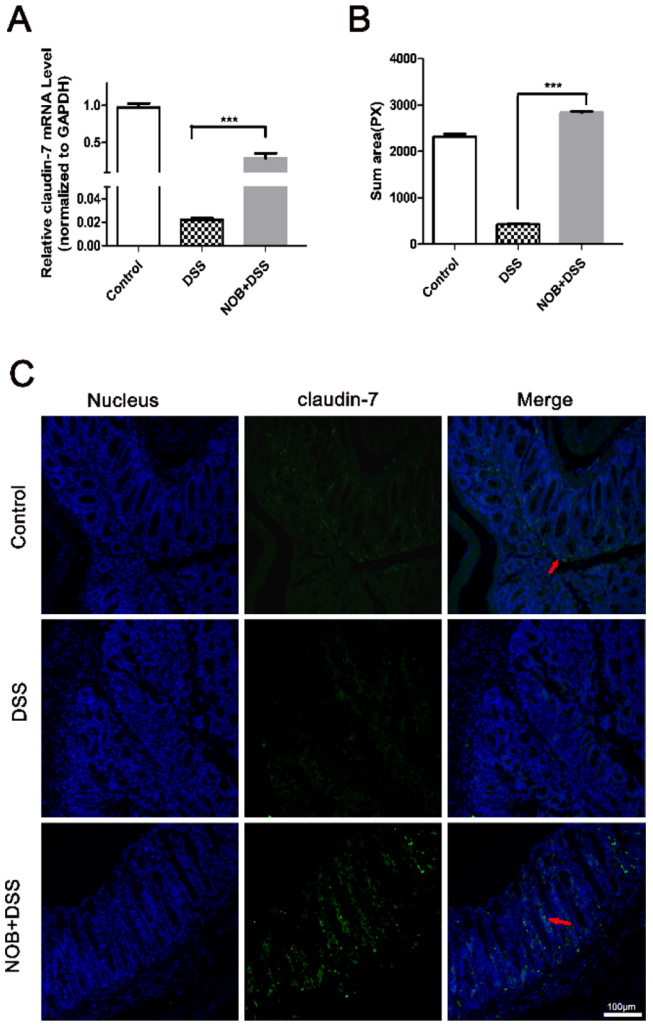

Figure 3. NOB increased the expression of claudin-7 in mouse colon. (A) mRNA levels of claudin-7 of observed groups were analyzed in the colon on day 7 ($n = 6$). Values were normalized to the value of GAPDH; (B) immunofluorescence was used to assess the distribution of claudin-7 in the colon. Images of stained for claudin-7 (green) and nuclei (blue). Scale bar, 100 μm. Red arrows indicate the expression of claudin-7 in colon villi; (C) statistical area of claudin-7 expression in terms of immunofluorescence intensity. DSS concentration is 3% (0.6–0.8 mM), NOB concentration is 0.25 mmol NOB in 1 kg of diet or 0.01% (wt/wt). All error bars represent SEM (***$P < 0.001$).

in the wild-type HT-29 cells that had been treated with NOB for 6 h. However, in HNF-4α-knockdown HT-29 cells, NOB stimulation did not lead to the increase of claudin-7 mRNA levels (Figure 6A). This observation indicated that NOB treatment is linked to the mRNA expression of claudin-7 in colon cells; therefore, we sought to determine whether NOB is involved in the transcriptional regulation of claudin-7. By means of the wild-type claudin-7 luciferase reporter construct, we noted that the fluorescence signaling of claudin-7 was weakened upon inflammatory stimulation and that this weakening was reversed by NOB addition (Figure 6B). Furthermore, we investigated whether HNF-4α served as a mediator of claudin-7 expression and NOB. Indeed, the upregulated luciferase activity of the claudin-7 reporter construct induced by NOB was strongly counteracted in HT-29 cells with HNF-4α knocked down (Figure 6C).

https://dx.doi.org/10.1021/acs.jafc.0c01217
J. Agric. Food Chem. 2020, 68, 4641–4649

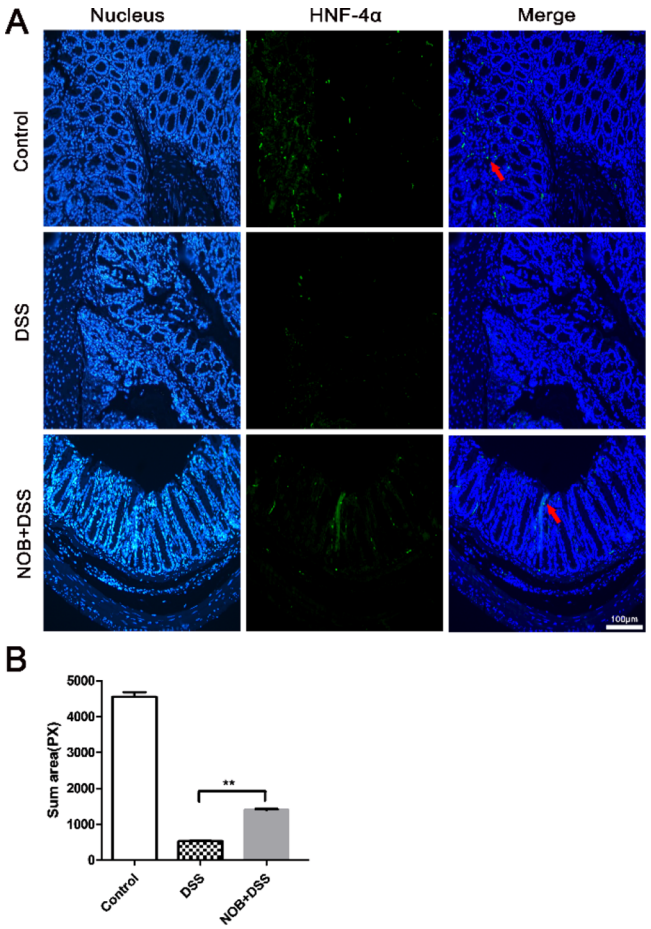

Figure 4. Modulation of claudin-7 by HNF-4α was involved the intestinal protection conferred by NOB. (A) Expression of HNF-4α in mouse colon. Images of colon villi stained for HNF-4α (green) and nuclei (blue). Scale bar, 100 μm. Red arrows indicate the expression of HNF-4α in colon villi. (B) Statistical area of HNF-4α expression in terms immunofluorescence intensity. DSS concentration is 3% (0.6–0.8 mM), NOB concentration is 0.25 mmol NOB in 1 kg of diet or 0.01% (wt/wt). All error bars represent SEM (**P < 0.01).

Given the well-established reports showing that HNF-4α transcriptionally regulates claudin-7 in colon cells,[4] we performed proof-of-concept assays to confirm that this regulatory mechanism can be used as a basis to understand our findings. Accordingly, a ChIP assay was performed to determine whether HNF-4α interacts with the claudin-7 promoter. Similar to a previous report,[4] our analysis of the putative binding sites of HNF-4α revealed that the HNF-4α antibody coprecipitated with the first binding site of the claudin-7-specific promoter DNA. Interestingly, the addition of NOB resulted in a higher level of coprecipitated claudin-7 promoter DNA than inflammatory stimulation alone (TNF-α plus LPS, Figure 6D,E). These observations suggest that NOB stimulation may affect the occupation of HNF-4α on the claudin-7 promoter in colon cells. To further confirm the association between HNF-4α and the claudin-7 promoter, a panel of luciferase reporter constructs was introduced into colon HT 29 cells. Consistently, the claudin-7 luciferase reporter construct cotransfected with a construct with mutated HNF-4α binding sites (named mut1 + 2) showed decreased transactivation by ~80%, as standardized with the value of the wild-type construct (Figure 6F) and left no doubt that HNF-4α was more influential than either mut1 (by ~45%) or mut2 (by ~50%). These findings indicated the transcriptional regulation of claudin-7 by HNF-4α.

We further added the double-labeling immunofluorescence combined with CLSM observation which can find the two proteins' co-location in mouse colon and to find their related signal pathways. As illustrated in Figure 7A, claudin-7 (green) is mainly expressed on the cell membrane and HNF-4α (red) on the nucleus. It can be seen from Figure 7B that DSS does reduce the expression of claudin-7 and HNF-4α, and the addition of NOB can significantly reverse this phenomenon. In addition, we also found that the expression of claudin-7 is proportional to HNF-4α, that is, where the expression of HNF-4α is high, the expression of claudin-7 is also high.

Taken together, these findings suggested that the NOB treatment protected the mice against DSS-induced intestinal injury and that these results may be attributed to the transcriptional regulation of claudin-7 by HNF-4α.

DISCUSSION

The intestinal epithelial barrier is constantly challenged by food intake, which is inevitably accompanied by foodborne toxins such as pathogenic microorganisms, heavy metal ions, allergens, and chemical molecules in addition to nutrients. Thus, maintaining intestinal integrity, including TJ integrity, provides physical barriers to favor nutrient absorption while minimizing risk factors, including those induced by harmful foreign materials and organisms infiltrating the body.[28] Notably, inflamed gut mucosa results in a destroyed intestinal barrier and then bacterial translocation and inflammatory mediator penetration. Hence, developments of products that strengthen

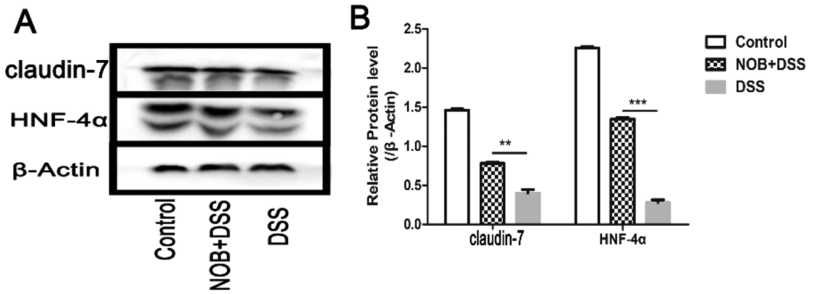

Figure 5. Modulation of claudin-7 by HNF-4α was involved the intestinal protection conferred by NOB. (A) Western blotting analysis of claudin-7 and HNF-4α proteins expression in colon tissue. (B) Relative protein expression is expressed as the fold increase after being normalized to β-actin in three independent experiments. DSS concentration is 3% (0.6–0.8 mM), NOB concentration is 0.25 mmol NOB in 1 kg of diet or 0.01% (wt/wt). All error bars represent SEM (**P < 0.01; ***P < 0.001).

https://dx.doi.org/10.1021/acs.jafc.0c01217
J. Agric. Food Chem. 2020, 68, 4641–4649

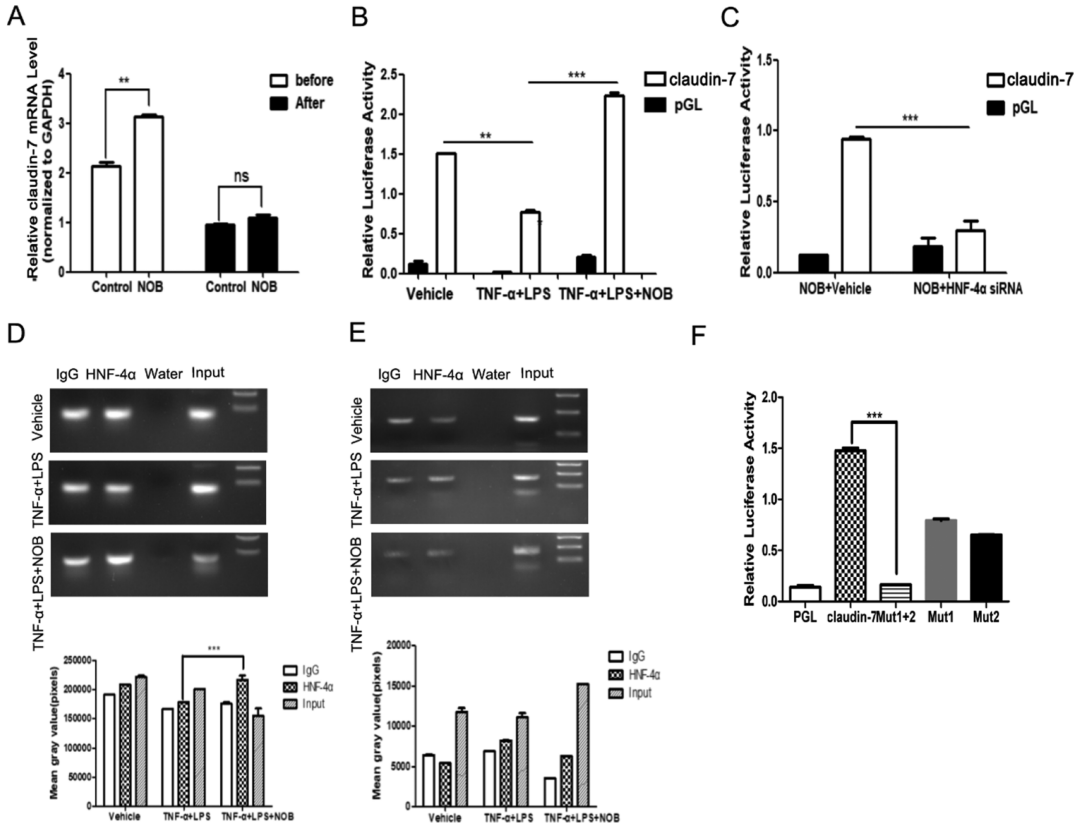

Figure 6. HNF-4α regulation of claudin-7 is involved in protective effects of NOB in colon cells. (A) In NOB-treated and non-treated cells, detect changes in RNA levels of claudin-7 before and after HNF-4α-knockdown. NOB failed to increase claudin-7 expression in the HNF-4α-knockdown HT-29 cells through specific siRNA. Before normal HT-29 cells; After HNF-4α-knockdown HT-29 cells; (B) HT-29 cells were treated with NOB/vehicle prior to TNF-α and IL-1β, the relative luciferase activity was tested in wild-type claudin-7 luciferase reporter construct. NOB reversed the downregulation of claudin-7 luciferase activity induced by inflammatory stimulation (TNFα plus LPS); (C) changes of luciferase activity in claudin-7 reporter construct before and after knocking down HNF-4α under NOB treatment. Loss of HNF-4α function in HT-29 cells blunted the upregulated claudin-7 transcription activity induced by NOB; (D) ChIP assay was used to examine the first putative binding site (−2519 bp) of HNF-4α on the claudin-7 promoter in HT-29 cells. The results indicated that the administration of NOB led to higher levels of precipitated promoter DNA; (E) second putative binding site (−856 bp) was examined in HT-29 cells, the precipitation efficiency of the second site is significantly lower than that of the first site; (F) claudin-7 promoter activity was substantially decreased when both HNF-4α binding motifs were mutated simultaneously (mut1 + 2). All error bars represent SEM (**P < 0.01; ***P < 0.001).

intestinal integrity are not only good for gut health but also good for the whole body.

In intestinal epithelium, TJs modulate diverse adhesive and polarity properties to establish selective paracellular permeability upon exposure to various stimuli.[26] For claudin-7, the identified target here is distributed along nearly the whole intestinal tract axis from stomach to colon.[29] Functionally, claudin-7 regulates extracellular matrix interactions, homeostasis, and differentiation.[25,30] The intestine-specific loss of claudin-7 initiates disruption of the mucosal barrier.[25,31] In addition, clinical evidence suggests that the level of claudin-7 protein appeared to be reduced in the colonic mucosa of IBD patients.[32,33] Accordingly, targeting the protection of claudin-7 represents a potential protective treatment of the intestinal barrier. Increasing evidence suggests that dietary plants and phytochemicals are linked intestinal mucosa protection.[34,35] Our present study aligns with this contention, as it showed that the administration of NOB diminished DSS-induced intestinal injury and remarkably increased claudin-7 levels in mouse intestine.

Throughout history, aged tangerine peels have been widely available among foods and herbs used in traditional Chinese medicine. PMFs are characteristic constituents of citrus peels, particularly rich in aged tangerine peels, in which NOB is the most abundant PMF phytochemical. NOB has a fundamental C6−C3−C6 skeleton in a three-ring system with multiple methoxy groups hence meets the conventional flavonoid definition.[7] The bioactivities of NOB, including intestinal protection, have been documented.[15,29,30] Inspired by our observation of NOB, in counteracting DSS-induced intestinal injury, we investigated further and found that a HNF4α-claudin-7 molecular cascade is the common target shared by NOB in their effects on the intestine barrier.

Interestingly, nuclear receptor HNF-4α in intestinal epithelial cells regulates claudin-7 expression during the epithelial differentiation process and homeostasis.[4] Moreover, HNF-4α has been identified, in many cases, as protective molecule for intestinal protection. For example, the HNF-4α level was significantly reduced in intestinal biopsy samples from patients with ulcerative colitis and Crohn's disease, and a mouse model suggested that HNF-4α protected the gut against DSS-induced intestinal injury.[36] HNF-4α drives Na^+/H^+ exchanger isoform 3 (NHE3) basal expression in the intestine to prevent the diarrhoea associated with inflammatory bowel disease.[37] Here, analyses of colon biopsy samples from mice indicated a positive correlation between HNF-4α and claudin-7. Additionally,

https://dx.doi.org/10.1021/acs.jafc.0c01217
J. Agric. Food Chem. 2020, 68, 4641−4649

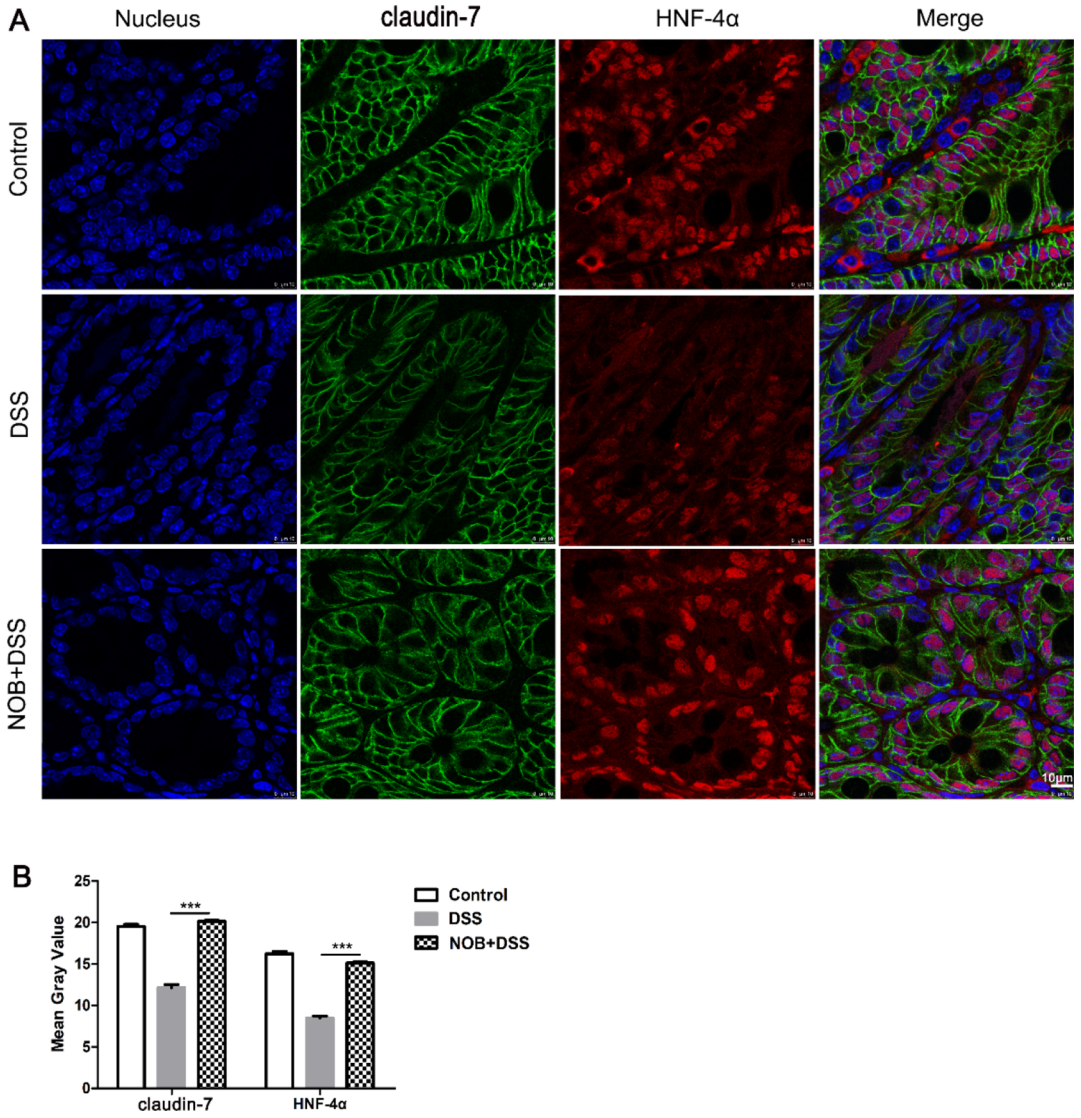

Figure 7. Increased claudin-7 promoter activity upon NOB stimulation was mediated by nuclear receptor HNF-4. (A) Claudin-7 and HNF-4α proteins' colocations were observed in mouse colon by the double-labelling immunofluorescence. Claudin-7 (green) is mainly expressed on the cell membrane, and HNF-4α (red) is mainly expressed on the nucleus. It can be seen from the figure that DSS does reduce the expression of claudin-7 and HNF-4α, and the addition of NOB can significantly reverse this phenomenon. Nucleus, blue. Scale bar, 10 μm. (B) Mean gray value of each group was measured by using ImageJ software. DSS concentration is 3% (0.6−0.8 mM), NOB concentration is 0.25 mmol NOB in 1 kg of diet or 0.01% (wt/wt). Data are reported in the mean ± SD (n = 3). All error bars represent SEM (***P < 0.001).

increased HNF-4α-induced claudin-7 expression contributed to the effects of NOB in the alleviation of the pathological severity of inflamed colon.

■ ASSOCIATED CONTENT

Supporting Information

The Supporting Information is available free of charge at https://pubs.acs.org/doi/10.1021/acs.jafc.0c01217.

Information of regents or resources; primers used in this study; toxicity study of NOB; ALT and AST levels in the serum of the mice were tested to determine whether NOB had a toxic effect; NOB decreased the iNOS expression in mice colon; TEER values examined in caco-2 cells; construction of claudin-7 expression vectors; and specific primers for mutations of two HNF-4α sites (PDF)

■ AUTHOR INFORMATION

Corresponding Authors

Hui Zhao − *Tianjin Key Laboratory of Food and Biotechnology, State Experimental and Training Centre of Food and Drug, School of Biotechnology and Food Science, Tianjin University of Commerce, Tianjin 300134, China;* orcid.org/0000-0002-3710-3607; Phone: 86-15022266054; Email: zhaohui@tjcu.edu.cn; Fax: 22-26686254

Meiyan Wang − *Tianjin Key Laboratory of Food and Biotechnology, State Experimental and Training Centre of Food and Drug, School of Biotechnology and Food Science, Tianjin University of Commerce, Tianjin 300134, China;* orcid.org/0000-0001-7914-3060; Email: wangmeiyan@tjcu.edu.cn

Shiming Li − *Hubei Key Laboratory of EFGIR, Huanggang Normal University, Huanggang, Hubei 438000, China; Department of Food Science, Rutgers University, New Brunswick, New Jersey 07102, United States;* Phone: 1-973-919-3702; Email: shiming@rutgers.edu; Fax: 1-732-932-6776

https://dx.doi.org/10.1021/acs.jafc.0c01217
J. Agric. Food Chem. 2020, 68, 4641−4649

Authors

Xiang Wen − *Tianjin Key Laboratory of Food and Biotechnology, State Experimental and Training Centre of Food and Drug, School of Biotechnology and Food Science, Tianjin University of Commerce, Tianjin 300134, China;* orcid.org/0000-0002-4294-3635

Liwen Wang − *Tianjin Key Laboratory of Food and Biotechnology, State Experimental and Training Centre of Food and Drug, School of Biotechnology and Food Science, Tianjin University of Commerce, Tianjin 300134, China*

Liang Wang − *Tianjin Key Laboratory of Food and Biotechnology, State Experimental and Training Centre of Food and Drug, School of Biotechnology and Food Science, Tianjin University of Commerce, Tianjin 300134, China*

Gang Du − *Tianjin Key Laboratory of Food and Biotechnology, State Experimental and Training Centre of Food and Drug, School of Biotechnology and Food Science, Tianjin University of Commerce, Tianjin 300134, China*

Wenqiang Guan − *Tianjin Key Laboratory of Food and Biotechnology, State Experimental and Training Centre of Food and Drug, School of Biotechnology and Food Science, Tianjin University of Commerce, Tianjin 300134, China*

Jianfu Liu − *Tianjin Key Laboratory of Food and Biotechnology, State Experimental and Training Centre of Food and Drug, School of Biotechnology and Food Science, Tianjin University of Commerce, Tianjin 300134, China*

Xiaocang Cao − *Department of Gastroenterology and Hepatology, General Hospital, Tianjin Medical University, Tianjin 300020, China*

Xiaohua Jiang − *Department of Histlolgy and Embrylolgy, School of Basic Medicine, North China University of Science and Technology, Tangshan, Hebei 063210, China*

Jingrui Tian − *Department of Histlolgy and Embrylolgy, School of Basic Medicine, North China University of Science and Technology, Tangshan, Hebei 063210, China*

Chi-Tang Ho − *Department of Food Science, Rutgers University, New Brunswick, New Jersey 07102, United States*

Complete contact information is available at: https://pubs.acs.org/10.1021/acs.jafc.0c01217

Author Contributions

In summary, our study demonstrated important conceptual advances that aged tangerine peels, and specifically, its bioactive compound NOB, prevent against DSS-induced intestinal epithelial injury. The involvement of the HNF4α-claudin-7 pathway may contribute to understanding the molecular mechanisms of PMFs from aged tangerine peels in remodeling the damaged intestinal barrier. These data support a further development of aged tangerine peel-based dietary nutraceuticals for improvement of intestinal barrier integrity and associated diseases.

Funding

This study was supported by the National Natural Science Foundation of China (grant nos. 31571832, 31772019, and 81803548), Tianjin Innovative Research Team grant (TD13-5087), Natural Science Foundation of Tianjin (19JCQNJC12400), Open Project of Tianjin Key Laboratory of Food Biotechnology (TJCU-KLFB-18201), and College Student Innovation and Entrepreneurship Training (201910069164).

Notes

The authors declare no competing financial interest.

ACKNOWLEDGMENTS

The authors would like to acknowledge Prof. Zongjin Li and Dr. Yitao Duan from Nankai University for their aid in the pathological assessment and construction of the luciferase reporter vectors and Yueying Wang, from the Institute of Radiation Medicine, Peking Union Medical College, for her guidance in the mouse experiments.

REFERENCES

(1) Dokladny, K.; Zuhl, M. N.; Moseley, P. L. Intestinal epithelial barrier function and tight junction proteins with heat and exercise. *J. Appl. Physiol.* **2016**, *120*, 692−701.

(2) Spadoni, I.; Fornasa, G.; Rescigno, M. Organ-specific protection mediated by cooperation between vascular and epithelial barriers. *Nat. Rev. Immunol.* **2017**, *17*, 761−773.

(3) Zhang, Y.; Zhou, S.; Deng, F.; Chen, X.; Wang, X.; Wang, Y.; Zhang, H.; Dai, W.; He, B.; Zhang, Q.; Wang, X. The function and mechanism of preactivated thiomers in triggering epithelial tight junctions opening. *Eur. J. Pharm. Biopharm.* **2018**, *133*, 188−199.

(4) Farkas, A. E.; Hilgarth, R. S.; Capaldo, C. T.; Gerner-Smidt, C.; Powell, D. R.; Vertino, P. M.; Koval, M.; Parkos, C. A.; Nusrat, A. HNF4α Regulates Claudin-7 Protein Expression during Intestinal Epithelial Differentiation. *Am. J. Pathol.* **2015**, *185*, 2206−2218.

(5) Xing, T.; Benderman, L. J.; Sabu, S.; Parker, J.; Yang, J.; Lu, Q.; Ding, L.; Chen, Y. Tight junction protein Claudin-7 is essential for intestinal epithelial stem cell self-renewal and differentiation. *Cell. Mol. Gastroenterol. Hepatol.* **2019**, DOI: 10.1016/j.jcmgh.2019.12.005.

(6) Yang, G.; Lin, C.-C.; Yuan, L.; Wang, P.; Yang, Y.; Wen, X.; Zhao, H.; Ho, C.-T.; Li, S. Nobiletin prevents TMAO-induced vascular oxidative stress in rats. *J. Food Bioact.* **2019**, *5*, 131−135.

(7) Li, S.; Wang, H.; Guo, L.; Zhao, H.; Ho, C.-T. Chemistry and bioactivity of nobiletin and its metabolites. *J. Funct. Foods* **2014**, *6*, 2−10.

(8) Zhang, H.; Zheng, J.; Liu, A.; Xiao, H.; He, L. Label-free imaging and characterization of cancer cell responses to polymethoxyflavones using raman microscopy. *J. Agric. Food Chem.* **2016**, *64*, 9708−9713.

(9) Wang, L.; Wang, J.; Fang, L.; Zheng, Z.; Zhi, D.; Wang, S.; Li, S.; Ho, C. T.; Zhao, H. Anticancer activities of citrus peel polymethoxyflavones related to angiogenesis and others. *BioMed Res. Int.* **2014**, *2014*, 1.

(10) Zhang, N.; Wei, W. Y.; Yang, Z.; Che, Y.; Jin, Y. G.; Liao, H. H.; Wang, S. sha; Deng, W.; Tang, Q. Z. Nobiletin, a polymethoxy flavonoid, protects against cardiac hypertrophy induced by pressure-overload via inhibition of napdh oxidases and endoplasmic reticulum stress. *Cell. Physiol. Biochem.* **2017**, *4*, 1313−1325.

(11) Harima-Mizusawa, N.; Kano, M.; Nozaki, D.; Nonaka, C.; Miyazaki, K.; Enomoto, T. Citrus juice fermented with lactobacillus plantarum YIT 0132 alleviates symptoms of perennial allergic rhinitis in a double-blind, placebo-controlled trial. *Benefic. Microbes* **2016**, *7*, 649−658.

(12) He, W.; Liu, M.; Li, Y.; Yu, H.; Wang, D.; Chen, Q.; Chen, Y.; Zhang, Y.; Wang, T. Flavonoids from Citrus aurantium ameliorate tnbs-induced ulcerative colitis through protecting colonic mucus layer integrity. *Eur. J. Pharmacol.* **2019**, *857*, 172456.

(13) Hagenlocher, Y.; Gommeringer, S.; Held, A.; Feilhauer, K.; Köninger, J.; Bischoff, S. C.; Lorentz, A. Nobiletin acts anti-inflammatory on Murine IL-10−/− colitis and human intestinal fibroblasts. *Eur. J. Nutr.* **2018**, *58*, 1391.

(14) Wu, X.; Song, M.; Gao, Z.; Sun, Y.; Wang, M.; Li, F.; Zheng, J.; Xiao, H. Nobiletin and its colonic metabolites suppress colitis-associated colon carcinogenesis by down-regulating iNOS, inducing antioxidative enzymes and arresting cell cycle progression. *J. Nutr. Biochem.* **2017**, *42*, 17−25.

(15) Xiong, Y.; Chen, D.; Yu, C.; Lv, B.; Peng, J.; Wang, J.; Lin, Y. Citrus nobiletin ameliorates experimental colitis by reducing inflammation and restoring impaired intestinal barrier function. *Mol. Nutr. Food Res.* **2015**, *59*, 829−842.

(16) Zhang, L.; Zhao, H.; Zhang, X.; Chen, L.; Zhao, X.; Bai, X.; Zhang, J. Nobiletin protects against cerebral ischemia via activating the p-Akt, p-CREB, BDNF and Bcl-2 pathway and ameliorating BBB permeability in rat. *Brain Res. Bull.* **2013**, *96*, 45−53.
(17) Li, S.; Lambros, T.; Wang, Z.; Goodnow, R.; Ho, C.-T. Efficient and scalable method in isolation of polymethoxyflavones from orange peel extract by supercritical fluid chromatography. *Journal of Chromatography B* **2007**, *846*, 291−297.
(18) Deguchi, Y.; Andoh, A.; Inatomi, O.; Yagi, Y.; Bamba, S.; Araki, Y.; Hata, K.; Tsujikawa, T.; Fujiyama, Y. Curcumin prevents the development of dextran sulfate sodium (DSS)-induced experimental colitis. *Dig. Dis. Sci.* **2007**, *52*, 2993−2998.
(19) Tanaka, K.-I.; Namba, T.; Arai, Y.; Fujimoto, M.; Adachi, H.; Sobue, G.; Takeuchi, K.; Nakai, A.; Mizushima, T. Genetic evidence for a protective role for heat shock factor 1 and heat shock protein 70 against colitis. *J. Biol. Chem.* **2007**, *282*, 23240−23252.
(20) Wang, J.; Yao, M.; Wang, Y.; Ho, C.-T.; Li, S.; Shi, Y.; Liu, Q.; Zhao, H. 6-Shogaol ameliorates injury to the intestinal mucosa and increases survival after high-dose abdominal irradiation. *J. Funct. Foods* **2017**, *36*, 63−71.
(21) Wu, J.; Li, M.; He, J.; Lv, K.; Wang, M.; Guan, W.; Liu, J.; Tao, Y.; Li, S.; Ho, C.-T.; Zhao, H. Protective Effect of pterostilbene on concanavalin a-induced acute liver injury. *Food Funct.* **2019**, *10*, 7308−7314.
(22) Yang, G.; Lin, C.-C.; Yang, Y.; Yuan, L.; Wang, P.; Wen, X.; Pan, M.-H.; Zhao, H.; Ho, C.-T.; Li, S. Nobiletin Prevents Trimethylamine Oxide-Induced Vascular Inflammation via Inhibition of the NF-κB/MAPK Pathways. *J. Agric. Food Chem.* **2019**, *67*, 6169−6176.
(23) Günzel, D.; Yu, A. S. L. Claudins and the Modulation of Tight Junction Permeability. *Physiol. Rev.* **2013**, *93*, 525.
(24) Farkas, A. E.; Capaldo, C. T.; Nusrat, A. Regulation of epithelial proliferation by tight junction proteins. *Ann. N.Y. Acad. Sci.* **2012**, *1258*, 115−124.
(25) Ding, L.; Lu, Z.; Foreman, O.; Tatum, R.; Lu, Q.; Renegar, R.; Cao, J.; Chen, Y. H. Inflammation and disruption of the mucosal architecture in Claudin-7-deficient mice. *Gastroenterology* **2012**, *142*, 305−315.
(26) Boivin, F. J.; Schmidt-Ott, K. M. Transcriptional mechanisms coordinating tight junction assembly during epithelial differentiation. *Ann. N.Y. Acad. Sci.* **2017**, *1397*, 80−99.
(27) Capaldo, C. T.; Powell, D. N.; Kalman, D. Layered defense: How mucus and tight junctions seal the intestinal barrier. *J. Mol. Med.* **2017**, *95*, 927−934.
(28) Rescigno, M. The Intestinal epithelial barrier in the control of homeostasis and immunity. *Trends Immunol.* **2011**, *32*, 256−264.
(29) Garcia-Hernandez, V.; Quiros, M.; Nusrat, A. Intestinal epithelial claudins: Expression and regulation in homeostasis and inflammation. *Ann. N.Y. Acad. Sci.* **2017**, *1397*, 66−79.
(30) Luissint, A.-C.; Parkos, C. A.; Nusrat, A. Inflammation and the intestinal barrier: Leukocyte-epithelial cell interactions, cell junction remodeling, and mucosal repair. *Gastroenterology* **2016**, *151*, 616−632.
(31) Tanaka, H.; Takechi, M.; Kiyonari, H.; Shioi, G.; Tamura, A.; Tsukita, S. Intestinal deletion ofClaudin-7enhances paracellular organic solute flux and initiates colonic inflammation in mice. *Gut* **2015**, *64*, 1529−1538.
(32) Stio, M.; Retico, L.; Annese, V.; Bonanomi, A. G. Vitamin D Regulates the tight-junction protein expression in active ulcerative colitis. *Scand. J. Gastroenterol.* **2016**, *51*, 1193−1199.
(33) Huang, Y.-Y.; Wang, Z.-K.; Li, J.; Bai, S.-W.; Shen, B.; Du, J.; Xia, X.-M.; Wang, F.-Y. The Effect of serine phosphorylated Claudin-7 on the epithelial barrier and the modulation by transient receptor potential Vanilloid 4 in human colonic cells. *Biomed. Pharmacother.* **2018**, *108*, 540−546.
(34) Bernardi, S.; Del Bo', C.; Marino, M.; Gargari, G.; Cherubini, A.; Andrés-Lacueva, C.; Hidalgo-Liberona, N.; Peron, G.; González-Dominguez, R.; Kroon, P.; et al. Polyphenols and Intestinal permeability: Rationale and future perspectives. *J. Agric. Food Chem.* **2019**, *68*, 1816.
(35) Peron, G.; Hidalgo-Liberona, N.; González-Domínguez, R.; Garcia-Aloy, M.; Guglielmetti, S.; Bernardi, S.; Kirkup, B.; Kroon, P. A.; Cherubini, A.; Riso, P.; Andrés-Lacueva, C. Exploring the molecular pathways behind the effects of nutrients and dietary polyphenols on gut microbiota and intestinal permeability: A perspective on the potential of metabolomics and future clinical applications. *J. Agric. Food Chem.* **2019**, *68*, 1780−1789.
(36) Ahn, S.-H.; Shah, Y. M.; Inoue, J.; Morimura, K.; Kim, I.; Yim, S.; Lambert, G.; Kurotani, R.; Nagashima, K.; Gonzalez, F. J.; et al. Hepatocyte nuclear factor 4α in the intestinal epithelial cells protects against inflammatory bowel disease. *Inflammatory Bowel Dis.* **2008**, *14*, 908−920.
(37) Muthusamy, S.; Jeong, J. J.; Cheng, M.; Bonzo, J. A.; Kumar, A.; Gonzalez, F. J.; Borthakur, A.; Dudeja, P. K.; Saksena, S.; Malakooti, J. Hepatocyte nuclear factor 4α regulates the expression of intestinal epithelial Na+/H+ exchanger isoform 3. *Am. J. Physiol.: Gastrointest. Liver Physiol.* **2018**, *314*, G14−G21.

https://dx.doi.org/10.1021/acs.jafc.0c01217
J. Agric. Food Chem. 2020, 68, 4641−4649